



HAL
open science

High-Chroma Color Coatings Based on Ag/SiO₂/Ti/SiO₂ Structures

Riley Shurvinton, Fabien Lemarchand, Antonin Moreau, Julien Lumeau

► **To cite this version:**

Riley Shurvinton, Fabien Lemarchand, Antonin Moreau, Julien Lumeau. High-Chroma Color Coatings Based on Ag/SiO₂/Ti/SiO₂ Structures. Advanced Photonics Research, In press, 10.1002/adpr.202200102 . hal-03819803

HAL Id: hal-03819803

<https://hal.science/hal-03819803>

Submitted on 18 Oct 2022

HAL is a multi-disciplinary open access archive for the deposit and dissemination of scientific research documents, whether they are published or not. The documents may come from teaching and research institutions in France or abroad, or from public or private research centers.

L'archive ouverte pluridisciplinaire **HAL**, est destinée au dépôt et à la diffusion de documents scientifiques de niveau recherche, publiés ou non, émanant des établissements d'enseignement et de recherche français ou étrangers, des laboratoires publics ou privés.

High-Chroma Color Coatings Based on Ag/SiO₂/Ti/SiO₂ Structures

Riley Shurvinton,* Fabien Lemarchand, Antonin Moreau, and Julien Lumeau*

A four-layer metal–dielectric–metal–dielectric (MDMD) stack design for color control is demonstrated. This stack incorporates Ag, SiO₂, and Ti as materials, enabling wide absorbance bands, high reflectance peaks, and a strongly tunable color. A wide gamut is obtained by varying the thickness of the SiO₂ cavity layer, and the resulting colors exhibit outstanding luminance and chroma. Coatings of red, green, and blue colors are designed and deposited. These coatings demonstrate a very close agreement between the simulated and experimental results. The chroma of the coatings is found to be similar to or exceeded the limits of the Pointer gamut, an empirical gamut of colors in reflectance. This shows that, in the generation of surface color, even for a simple four-layer stack, the performance of thin-film coatings can rival or exceed that of traditional paints and dyes.

1. Introduction

The use of nanostructured interference coatings for color generation is currently garnering increasing interest in research, commercial, and industrial applications. These coatings provide compelling advantages over traditional colorants (dyes or pigments), such as better resistance to degradation under temperature or UV light, which is crucial in applications such as color filters in displays.^[1] Precise control of the reflectance spectrum allows more “pure” colors to be obtained, such as extremely vivid blue^[2] or highly absorbing black.^[3] Thin-film coatings can produce attractive metallic colors^[4] or colors that shift depending on the viewing angle.^[5] Structures incorporating phase-change materials can allow active tunable colors, which is promising in technologies such as low-powered displays.^[6–8]

One common approach to color control is to use a thin-film coating incorporating metal–dielectric–metal (MDM) or metal–insulator–metal (MIM) stacks.^[9–12] Analogous to a Fabry–Perot cavity, the upper and lower metallic layers act as mirrors

surrounding a central cavity where light oscillates. At certain wavelengths, a standing wave forms inside the cavity, and losses from the semitransparent upper layer contribute to the perfect or near-perfect absorbance. The output of the stack can be further tailored with an additional layer on top to aid phase matching,^[13] creating a so-called MDMD (or MIMI) stack.


The key advantage of an MDMD stack is that it is simple to fabricate, in comparison to other structures that have been demonstrated to generate high chroma (such as the near-ideal red obtained by Dong et al. with Si nanoantennae,^[14] or the high-purity red and blue filters designed by Yang et al incorporating organic dye layers^[15]). The stack design is lithography-free and versatile enough to generate a wide range of colors. This may be achieved by changing the layer thickness and the choice of material, including most commonly cyan/magenta/yellow^[9,16–18] primaries. However, few of these approaches provide the ideal spectral features for color, which are generally not well understood within the thin-film community.

Certain colors, such as red, green, and blue primaries, present further challenges. Obtaining these colors requires the suppression of large parts of the visible spectrum and selective reflectance of only red, green, or blue light. Several prior studies have demonstrated RGB coatings in reflectance,^[19,20] and the spectra obtained are nonideal, with low peak reflectance (≈ 0.7 – 0.9), imperfect absorption at undesired wavelengths, and slowly varying spectral features leading to poorer color purity and lower perceptual chroma.

Taken together, these results suggest a potential for improvement: a single coating design that yields improved chroma, which can generate a wide range of colors simply by tuning the layer thicknesses. This desirable property of tunability increases the versatility of the coating and allows its viability for a range of applications. In addition, improving the chroma of the coatings will allow them to approach or even exceed the appearance and performance of the currently used dyes and pigments for a color generation.

To the best of our knowledge, the realization of the widest and highest chroma gamut obtained with a simple four-layer stack architecture has been presented herein. Furthermore, it is demonstrated that an MDMD stack incorporating Ag, SiO₂, and Ti yields high tunability and enables the generation of high-chroma coatings of almost any hue. The design principles to be followed have been described when selecting the layer thicknesses, informed by the spectral features of the theoretically ideal color reflector described by Ostwald and Schrödinger.^[21,22] A trio of

R. Shurvinton, F. Lemarchand, A. Moreau, J. Lumeau
CNRS
Centrale Marseille
Institut Fresnel
Aix Marseille Univ
13007 Marseille, France
E-mail: riley.shurvinton@univ-amu.fr; julien.lumeau@fresnel.fr

 The ORCID identification number(s) for the author(s) of this article can be found under <https://doi.org/10.1002/adpr.202200102>.

© 2022 The Authors. Advanced Photonics Research published by Wiley-VCH GmbH. This is an open access article under the terms of the Creative Commons Attribution License, which permits use, distribution and reproduction in any medium, provided the original work is properly cited.

DOI: 10.1002/adpr.202200102

red, green, and blue coatings was designed, and it was demonstrated that when deposited, these coatings show close agreement with the simulated spectra yielding appealing colors that are both bright and high-chroma. When assessed in comparison with the Pointer gamut, it was found that the coatings have near-ideal or better-than-ideal chroma compared to traditional pigments.

2. Design Principles for Creating Red, Green, and Blue Primaries

When working in the field of colors, it is first necessary to establish a coordinate system to provide meaning to and allow the specification of exact colors. First, the color system used in this work is briefly described, followed by an overview of other theoretical considerations, such as the spectral shape of a maximum-chroma pigment.

In this work, the word “chroma” is used to refer to the perceptual strength of a color (sometimes also called saturation). This is not to be confused with the xy coordinates of CIExyY color space, referred to as the “chromaticity coordinates.”

2.1. A Perceptual Color Space should be used to Accurately and Intuitively Describe Color and Chroma

Commonly, xy chromaticity coordinates are used to assess color saturation. They describe a combination of hue and white admixtures; thus, for some applications (such as transmission filters), these coordinates may be used as a measure of color purity. However, these are generally insufficient to describe perceptual chroma (used here to mean the “strength” of a color in reflectance), because they do not contain any information about the luminance of a color. In the limiting case, a coating that reflects only one wavelength has chromaticity coordinates identical to those of spectrally pure light, which appears to suggest a high chroma. However, in appearance, the color will be black with 0 chroma because it only reflects a vanishingly small portion of the incoming light under typical broadband illumination conditions (such as daylight or interior lighting). Evidently, in terms of reflectance, luminance has a large impact on the perceptual chroma of a surface.

Instead of xy coordinates, we propose the use of CIELAB to assess the color. CIELAB is a perceptual color space based on the color opponent-process theory,^[23,24] which is often used in industry to specify surface colors. It transforms the CIEXYZ triplet XYZ into three new coordinates: L^* (the perceptual luminance) and a^* and b^* , which are approximately representative of the red-green and yellow-blue color opposition axes. The coordinates are obtained using the following linear transforms^[25]

$$L^* = 116f\left(\frac{Y}{Y_n}\right) - 16 \quad (1)$$

$$a^* = 500\left(f\left(\frac{X}{X_n}\right) - f\left(\frac{Y}{Y_n}\right)\right) \quad (2)$$

$$b^* = 200\left(f\left(\frac{Y}{Y_n}\right) - f\left(\frac{Z}{Z_n}\right)\right) \quad (3)$$

where $t = \frac{X}{X_n}, \frac{Y}{Y_n}$ or $\frac{Z}{Z_n}$

$$f(t) = \begin{cases} \sqrt[3]{t} & \text{if } t < 3 \\ \frac{t}{36^2} + \frac{4}{29} & \text{otherwise} \end{cases} \quad (4)$$

$$\delta = \frac{6}{29}$$

$X_n, Y_n,$ and Z_n are whitepoint coordinates that depend on the illuminant. The difference ΔE between any two colors can be expressed by the Euclidean distance between them as follows

$$\Delta E_{\text{Lab}} = \sqrt{(\Delta L^*)^2 + (\Delta a^*)^2 + (\Delta b^*)^2} \quad (5)$$

The $L^* a^* b^*$ coordinates may be further transformed into cylindrical coordinates, HCL (representing the hue, chroma, and luminance of a color). The HCL coordinates have improved intuitive meaning, similar to the coordinates used in art or in the Munsell color space. $L = L^*$, and C and H are obtained as follows

$$C = \sqrt{a^{*2} + b^{*2}} \quad (6)$$

$$H = \arctan \frac{a^*}{b^*}$$

The chroma coordinate C is a superior measure of the perceptual chroma compared to the xy chromaticity coordinates. Instead of simply considering the admixture of the white color, the C coordinate also considers the perceptual brightness of the color. The space is not entirely and perfectly uniform (indeed, Pointer 1980^[26] notes that in the magenta range, at a hue angle of 325, “the gamuts [...] are] characterised by a ‘peak’ of high chroma [...] an artifact of the $L^* a^* b^*$ color space”). Nevertheless, it is an improved measure of chroma compared to the chromaticity coordinates. In the following paragraphs, we use the word “chroma” to refer to the coordinate C of a given color.

2.2. The Pointer Gamut Provides Guidelines for Maximal Chroma in Reflectance

There is a fundamental trade-off between luminance and chroma in reflectance. The closer a surface is to reflecting only a single wavelength, the lower its brightness, which reduces perceptual chroma. However, wideband reflectors also have low color purity because they reflect many different colors of light. The luminance at which the maximal chroma occurs differs depending on the hue because of the uneven sensitivity of the eye to different wavelengths of light.

This trade-off is expressed in the Pointer gamut,^[26] an empirical gamut obtained by measuring the surface colors of thousands of real-world samples including paint swatches, printing inks, and objects from nature. The gamut describes the maximum chroma of a set of measured samples for various hues and luminance. A plot of the Pointer gamut within the CIExy chromaticity diagram shows that the colors with maximum reflectance chroma occur fairly far from the maximal color purity (Figure 1).

Although more recent work has shown that the Pointer gamut does not completely cover all colors attainable in reflectance,^[27] it is well known as a baseline for describing colors in reflectance; therefore, it was used for comparison in this work. If the coordinates of our designed color coatings lie close to or on the

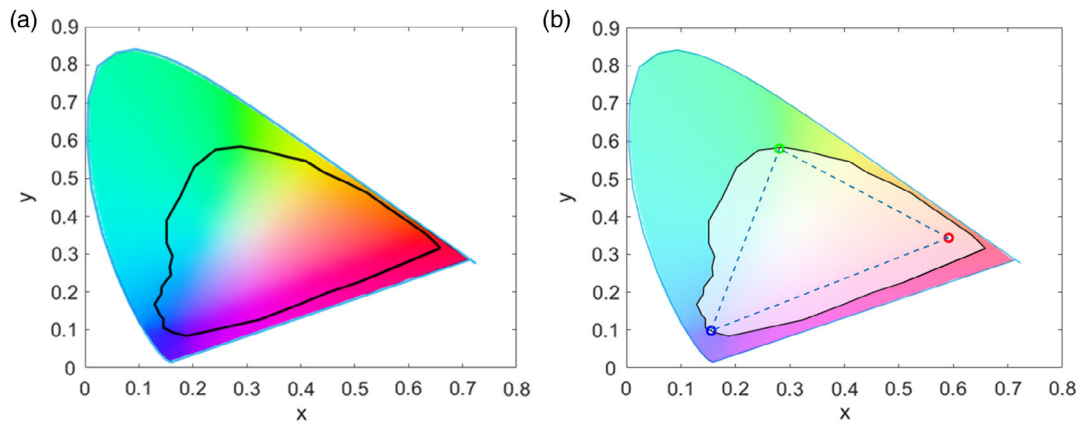


Figure 1. a) CIExy chromaticity diagram, showing the xy chromaticity coordinates for all colors visible for normal human vision (color rendering approximate). The interior solid black curve shows the Pointer gamut, an empirical measurement of surface colors in reflectance. b) CIExy coordinates of the red, green, and blue coatings (circles), shown against the Pointer gamut. The triangle between them shows the gamut of colors that can be obtained using combinations of the three coatings as additive primaries – for example, as RGB pixels in a reflective display. Coordinates measured/calculated under a CIE “C” illuminant.

boundary of the Pointer gamut, it indicates that excellent reflectance chroma has been achieved. Indeed, as the gamut is empirical and not theoretical, extremely high-chroma coatings can even exceed the limits of the Pointer gamut, providing a further advantage of nanostructured coatings over traditional pigments.

The original 1980 paper^[26] presented its findings in terms of the CIELUV color space, an alternative perceptual color space that is often used in computer graphics. The data provided here are taken from a spreadsheet made available by Pointer,^[28] which provides values both in CIELUV and CIELAB.

2.3. The Spectral Shape of a Reflector with Optimal Chroma is a Square Wave

When considering the trade-off between color purity and luminance, a reflector with an optimal chroma must maximize the reflectance over the desired wavelength range and minimize it elsewhere. These principles were first described by Ostwald and Schrödinger in the early 1900s.^[21,22] From theoretical considerations, Schrödinger showed that such an ideal pigment must have a reflectance of 1 or 0 throughout, with sharp transitions between them. Additionally, a maximum of two transition points must exist, resulting in either a single isolated reflectance peak (with perfect absorbance elsewhere) for most hues or a single isolated absorption band (with unity reflectance elsewhere) for colors in the magenta range. **Figure 2** shows schematic plots of the spectra of ideal pigments.

This provides guidance for the design of color coatings with a high chroma. Reflectance must be maximized over the desired wavelength range and minimized elsewhere, with the transitions between them as sharp as possible. Additionally, at most two reflectance peaks in the spectrum (for magenta colors) or one single peak for all other hues must be present. Therefore, sidebands and secondary resonance features are required to be suppressed as much as possible.

In practice, creating a coating with square-wave reflectance spectra (essentially a notch filter) is extremely difficult, requiring

tens or hundreds of layers with precisely controlled thicknesses. However, with careful material choices, an approximation of this spectrum may be approached using a simpler MDMD structure. Further improvements that can be made with a more complex stack design can then be assessed by comparing the chroma of the MDMD stack with that of the corresponding ideal reflector.

3. Design of MDMD Coatings

Having outlined the theoretical principles of color control, we proceed with a closer examination of the MDM/MDMD stack and demonstrate how it may be optimized to yield high-chroma colors.

3.1. Operation of an MDM Coating Analogous to a Fabry–Perot Resonator

The principle of operation of a MDM structure is analogous to that of an asymmetric Fabry–Perot resonator (see **Figure 3**). The lowermost layer of the coating is an opaque metallic layer, which acts as a mirror. Next, there is a cavity layer made of a dielectric material several hundred nanometers thick, followed by a second semitransparent metallic layer of a few tens of nanometers thickness, which acts as the upper mirror. At resonant wavelengths, strong absorbance exists, and elsewhere, the structure yields a high reflectance. These resonant wavelengths depend on the material and thickness of the layers. The resonance may also be tuned by an additional phase-matching dielectric layer on top of the upper mirror.

Recent studies, such as those by Z. Yang et al.,^[29] present a more in-depth theoretical overview of the impact of each layer considering a single central wavelength, where the reflectance is sought to be maximized. Here, we focus on the qualitative exploration of the impact of each layer, as there are several other spectral features that affect color realization (spectral width, absorption bandwidth), for which a full theoretical discussion will be extremely lengthy and outside the scope of this work.

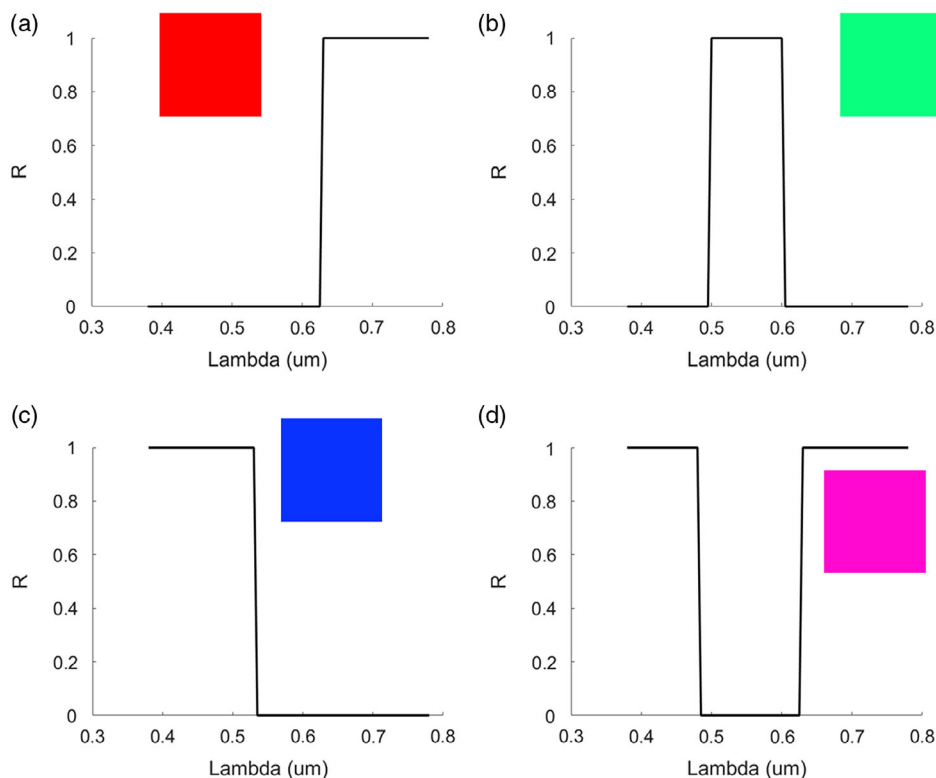


Figure 2. Example spectra of the four classes of bivalent pigments, as arranged by Schrodinger. a) Long-wavelength (red-range) pigments; b) middle-wavelength (green-range) pigments; c) short-wavelength (blue-range) pigments, and d) mid-absorbing (magenta-range) pigments. The optimal width of the spectral features to obtain maximum chroma varies strongly depending on the chosen hue, owing to the uneven sensitivity of the eye to different wavelengths of light. (Swatches do not accurately represent the pigment colors, and are for illustrative purposes only.).

3.2. Assessment of Material Choices in the MDMD Stack

3.2.1. Lower Layer Material Choice Changes Peak Reflectance

As described in Section 2.3, one of the requirements of an ideal pigment is a reflectance of 1 over the desired wavelength region. In practice, the closer the peak reflectance of a coating is to 1, the brighter and more luminant the coating appears, leading to a higher perceptual chroma. Therefore, for the lower layer of the MDM(D) stack, it is important to select a material with the highest reflectance possible. Al and Ag are the two materials most commonly used for this purpose, as they are both near-ideal metals with high reflectance in the visible range. In this study, Ag was selected because it has a higher reflectance than Al above ≈ 420 nm. However, Al has similar performance and may be preferable in some applications owing to factors such as cost, compatibility with other materials in the stack, and improved adhesion.

3.2.2. Central Cavity Thickness can be used to Tune Absorbance Bands

For the selection of the cavity layer material, both lossless dielectrics (such as SiO_2 ^[30] and TiO_2 ^[9]), and lossy semiconductors (such as Si ^[17,31] and Ge ^[13,32]) have been studied. Both choices have certain advantages and disadvantages.

MDM/MIM coatings employing lossy dielectrics, such as Si, are thinner and more angle-resistant than those using lossless dielectrics because of the large phase shift on reflectance at the layer interface obtained with a lossy material. Therefore, only a very thin layer is required to satisfy the resonance condition within the visible range of 380–780 nm. Conversely, 100+ nm of a lossless dielectric, such as SiO_2 , is required to fulfill this resonance condition, as the main contributions to the phase shift are from the optical path length, which depends on the layer thickness.

However, the absorbance of a lossy dielectric limits the thickness of the material that can be used without introducing significant losses and damaging the resonance to ≈ 50 nm for materials such as Si. For thicker layers, the losses drastically reduce the luminance and chroma of the resulting color. Therefore, this reduces the tunability of the stack, that is, the number of different colors that may be achieved by simply varying the thicknesses of the layers.

This can be observed when considering the gamut of achievable colors for an Ag/[dielectric]/Ti stack with either SiO_2 or Si as the dielectric when adjusting the dielectric thickness, as shown in Figure 3b–c. Although high-chroma colors can be realized in the violet-blue spectrum (with appreciable chroma into the yellows) for an Si layer, increasing the Si thickness further dramatically reduces the chroma, restricting the available gamut. In contrast, the use of SiO_2 allows a dielectric thickness of 500 nm or more to be used in the stack without damaging the color chroma, which

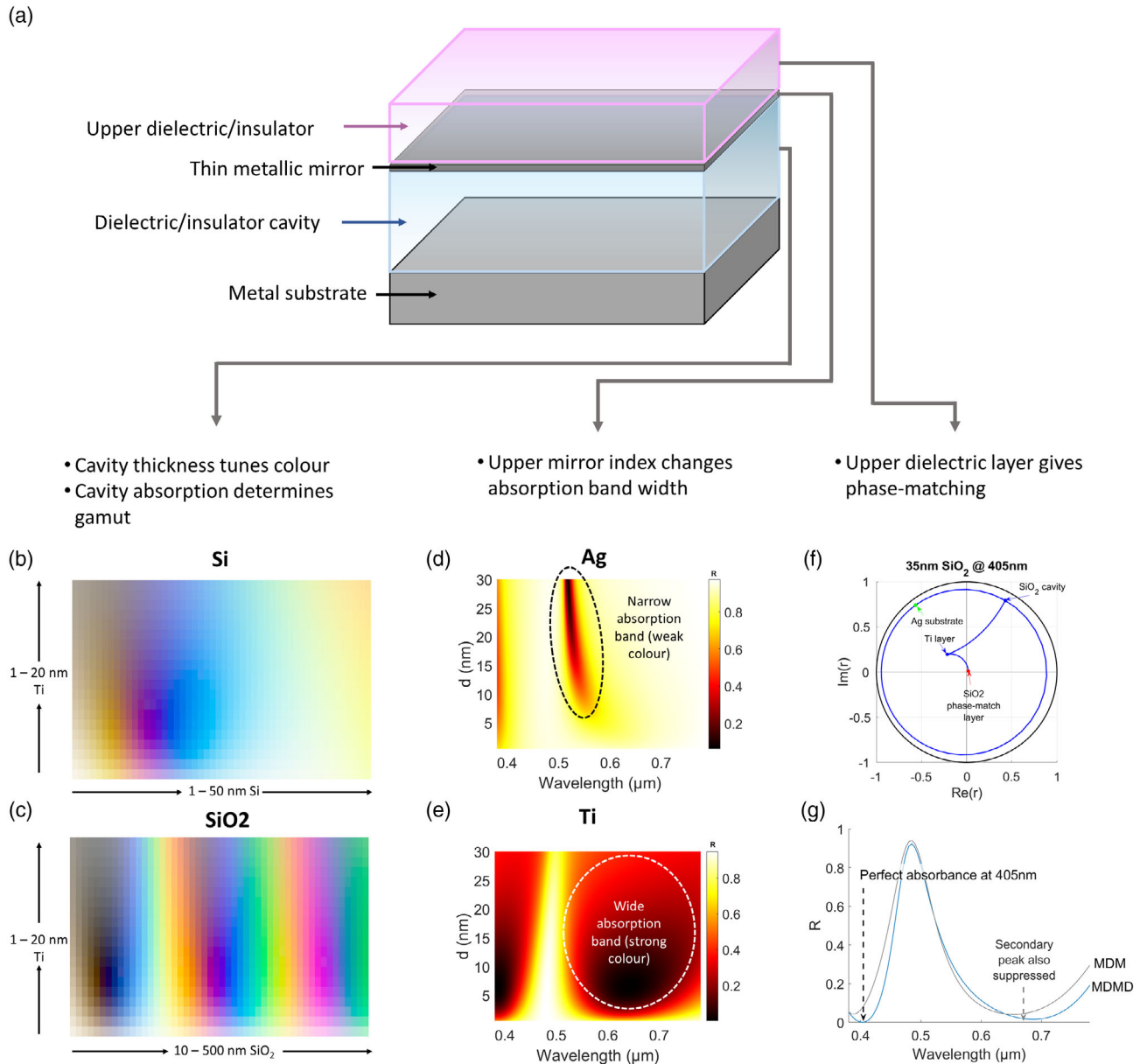


Figure 3. a) Schematic of an metal–dielectric–metal–dielectric (MDMD)/MIMI-type stack. The different layers have different impacts on the spectral response. b) An example gamut of an MDM stack using Ag/Si/Ti as the thicknesses of the Si and Ti layers are varied. The gamut of achievable high-chroma colors is restricted to yellow, magenta, and blue, with chroma strongly diminishing for thicker Si layers. c) An example gamut of an MDM stack using Ag/SiO₂/Ti as the thicknesses of the SiO₂ and Ti layers are varied. High-chroma colors of almost any hue may be obtained by varying the SiO₂ thickness. d,e) Plots showing the effect on reflectance spectrum for a stack of Ag/300 nm SiO₂/d nm absorber of increasing d, the thickness of the absorber layer. (d) The effect of an Ag layer of generating a very narrow absorption band, with high reflectance elsewhere. (e) The effect of a Ti layer, which generates wide absorption bands and a narrower reflectance peak. f) Plot of the evolution of the complex Fresnel coefficient r on an Ag/300 nm SiO₂/10 nm Ti/35 nm SiO₂ stack, from Ag substrate to added phase-matching SiO₂ layer. The phase-matching layer allows perfect absorbance to be achieved at $\lambda = 405$ nm with this stack. g) The effect of the upper phase-matching layer on the reflectance spectrum of the stack described in (f). Apart from achieving perfect absorbance at $\lambda = 405$ nm, the phase-matching layer has the effect of suppressing the secondary reflectance peak between 650 and 750 nm.

leads to an extremely wide gamut. Colors of almost any hue, with large chroma and brightness, can be obtained by varying the dielectric thickness. Thus, the output of the stack is highly tunable.

An additional important consideration is that using a lossless dielectric implies that the majority of the phase shift depends

on the optical path length. The path length varies with the angle of the incoming light, and therefore the resonance conditions – and thus, the resulting color – will also be strongly angle-dependent. This may be undesirable for some applications but can be exploited for other applications, such as sensors or camouflage technology.^[5]

The angle dependence may be reduced using a high-index lossless dielectric such as Ta₂O₅ and TiO₂. For more discussion regarding the angle- and polarization-dependent behavior, see Section 3 of the supporting information. However, in this study, only the coating appearance at near-normal incidence ($\approx 8^\circ$) was considered. As such, we chose SiO₂ as the dielectric material because its properties are well known for our deposition process.

3.2.3. Upper Mirror Material Choice Impacts the Broadness of the Absorption Bands

In a traditional Fabry–Perot resonator, an ideal metal (where $n \ll k$) is used for the top layer to minimize absorption losses. This results in the well-known series of narrow transmission (or, here, absorbance) bands, with high reflectance in between. A simulation of the reflectance of an asymmetric Fabry–Perot cavity with 300 nm SiO₂ and an upper Ag mirror shows that the absorbance band obtained is extremely narrow relative to the spacing, resulting in wide reflectance peaks with narrow regions of absorption between them (Figure 3d).

However, such a spectrum yields poor surface color.^[30] The multiple wide regions of high reflectance in the spectrum result in a wide range of wavelengths reflected by the coating. Thus, the color approaches that of a broadband reflector (i.e., white). To obtain a high-chroma reflectance color, a wider part of the absorbance spectrum must be suppressed to enable the generation of one or two narrower reflectance peaks. This can be achieved using a nonideal “lossy” metal to yield broader absorption bands.

Such a metal should have the property $n \approx k$. The exact optimal index for this metal depends on the wavelengths at which reflectance and absorption are desired.^[29] The use of a lossy material widens the spectral features of a cavity in a manner that is similar to the dependence of the output of a Fabry–Perot stack on the reflectivity of its mirrors. When a mirror with lower reflectivity is used (e.g., a nonideal, lossy metal), the Airy fringe distribution is broadened. Similarly, the use of a lossy metal as the upper mirror in an MDM stack creates broader absorption bands, which are well suited for generating saturated colors.

We propose Ti as a well-suited generic choice for this purpose, for three reasons. First, its index from 10 to 20 nm thickness is reasonably stable, unlike some metals which show large changes in refractive index for thin layers.^[12] Second, it has desirable index properties, $n \approx k \approx 2$, within the visible spectrum, with slow and smooth variation, allowing it to be applicable for the generation of many colors (unlike gold, which is only suitable for generating red–yellow-range colors). Third, a layer of ≈ 10 nm Ti on top of Ag/SiO₂ generates wide absorption bands without significantly diminishing the peak reflectance (Figure 3e).

In addition, our team thoroughly characterized its behavior on top of a layer of SiO₂ and well-calibrated the deposited thickness, demonstrating its compatibility with SiO₂.^[33]

3.2.4. Optional Upper Dielectric Layer Can Tune Color via Phase-Matching

The spectrum can be further tuned by the addition of a second SiO₂ layer on top. This layer serves two purposes: first, it protects

the upper metal (Ti) from oxidation. Additionally, when a suitable thickness is used (typically tens of nanometers), this layer further provides phase-matching that allows the absorbance to be adjusted and, in some cases, broadened.

For example, a stack of Ag/300 nm SiO₂/10 nm Ti has an absorbance band centered at approximately 390 nm, but perfect absorbance is not achieved ($R \approx 0.05$). Figure 3f shows the effect on the admittance at $\lambda = 405$ nm of adding an additional phase-matching layer of 35 nm SiO₂ on top of the stack. The Fresnel coefficient r is shifted from $-0.2 + 0.2i$ to ≈ 0 , indicating $R \approx 0$ at this wavelength (i.e., perfect absorbance is achieved at 405 nm). Figure 3g shows the effect of this additional layer on the reflectance spectrum of the coatings. The reflectance at 405 nm is shifted from ≈ 0.05 (gray curve) to 0 (blue curve) by the phase-matching layer. This layer also slightly suppresses the secondary reflectance peak between 650 and 750 nm. Thus, the color can be slightly tuned, and the purity and chroma can be enhanced using an upper dielectric layer in the stack.

3.3. A Tunable Stack Design Can Generate a Wide Range of Colors

Given the aforementioned results, we conclude that an MDMD structure based on Ag/SiO₂/Ti/SiO₂ is an efficient solution for generating color coatings. To illustrate the versatility of this stack, we calculated the gamut of colors obtained by varying the lower SiO₂ thickness from 10 to 500 nm, and the Ti thickness from 1 to 20 nm (Figure 3c). A wide range of hues was obtained within this gamut, with outstanding chroma and brightness when the appropriate layer thicknesses were chosen. As demonstrated, there is an option to further tune the color by adjusting the upper SiO₂ layer. Thus, colors of almost any hue with high chroma can be generated using this stack type, fulfilling the condition of high tunability.

To demonstrate this, we designed three coatings: red, green, and blue. Primary colors are desired in many applications, such as display technologies, and as they can be obtained with high luminance and chroma, they may be used to define a wide additive gamut. In addition, the realization of these colors with high chroma is technically demanding because it requires the suppression of reflectance over a large wavelength range within the visible spectrum. Obtaining these three colors with high chroma using this stack type is indicative of the versatility and tunability of the stack. The resulting formulas for the three coatings and their performances with regard to color are discussed in the next section.

4. Results and Discussion

4.1. Layer Thicknesses May Be Mathematically Optimized Within Given Bounds to Yield Maximal Chroma for a Fixed Hue

A key advantage of using an MDMD stack for color is that the design process is significantly simplified. After fixing the material choices, there are only three degrees of freedom for the stack design: the thicknesses of the upper and lower SiO₂ layers and the thickness of the Ti mirror. Therefore, the design process can

be simplified as a straightforward optimization procedure for these three variables.

For the design of the red, green, and blue primaries, a target hue angle was specified for each coating: 50 for the red coating, 130 for the green coating, and 310 for the blue coating (under CIE standard illuminant C, to allow comparison with the data from the Pointer gamut). The upper and lower tolerances of 5° were set for the hue because even a small change in hue can yield a large perceptual difference in color.

The starting point for the layer thicknesses was identified by observing the gamut. The initial SiO₂ cavity thicknesses were set to 230 nm for the red coating, 320 nm for the green coating, and 90 nm for the blue coating and optimized around these starting points with a tolerance of 50 nm on either side. A lower bound of 10 nm was set for the thickness of the Ti layer. For thinner layers, there may be concerns about inhomogeneity or a significant change in the optical properties of the layer. Based on initial simulations, an upper bound was set at 40 nm; above this thickness, absorption losses from the Ti layer diminished the color. The upper SiO₂ thickness was allowed to vary freely with a maximum thickness of 500 nm.

The thicknesses of all three layers were optimized to maximize the chroma of each coating within the hue tolerances under a C illuminant. The resulting formulas for the three coatings are listed in Table 1.

4.2. The Optimized MDMD Coatings Are Close to or Exceed the Limits of the Pointer Gamut in Chroma

The optimized chroma and luminance for the red, green, and blue coatings under a C illuminant are reported in Table 2. The luminance of each coating varies with hue because the luminance response of the eye is uneven; green hues appear more perceptually luminant than red or blue hues. All three coatings demonstrated high chroma. The lowest was the red coating, with a chroma of 83, and both the green and blue MDMD coatings demonstrated a chroma above 100 (108 and 104, respectively).

For interpretation, these values are compared to the equivalent values from the Pointer gamut – the empirically measured limits of surfaces in reflectance, consisting of paint samples and objects from nature. For the equivalent hue and luminance values, the chroma of the red MDMD coating (83) was close to the limit of the Pointer gamut (102). This indicates that the red MDMD coating is a fairly vibrant red color, although there may be some materials, such as very vibrant red paints, that exceed its chroma.

In comparison, both the green and blue MDMD coatings exceeded the limits of the Pointer gamut for equivalent hue and luminance. The blue MDMD coating demonstrated a chroma of 104 compared to the Pointer gamut limit of 85,

Table 1. Optimized MDMD coating designs for the red, green, and blue primaries.

Color	SiO ₂ Cavity Thickness [nm]	Ti layer thickness [nm]	Upper SiO ₂ thickness [nm]
Red	215	10	230
Green	330	10	190
Blue	110	10	130

Table 2. Hue, chroma, and luminance of the MDMD red, green, and blue coatings; the equivalent points on the pointer gamut (to the nearest 10 hue degrees/5 luminance units); and the equivalent ideal reflector with maximum chroma. Data calculated using CIE standard illuminant “C”.

Sample	Hue [°]	Chroma	Luminance
MDMD red	50	83	53
Pointer equiv.	50	102	55
“Ideal” red	50	123	55
MDMD green	129	108	83
Pointer equiv.	130	64	85
“Ideal” green	129	150	83
MDMD blue	312	104	24
Pointer equiv.	310	85	25
“Ideal blue”	314	175	23

and the green MDMD coating a chroma of 108, which is considerably larger than the Pointer gamut limit of 64. This indicates that both the green and blue MDMD coatings are far more vivid than any of the samples measured in the original Pointer gamut, providing bold and vibrant green and blue colors, respectively.

The same conclusions were drawn when the entire Pointer gamut for each hue was considered. Figure 4c–e shows chroma-luminance plots for each of the three hue angles. MDMD red is slightly below the peak chroma, but the MDMD green and blue coatings still yield greater chroma than that measured anywhere within the Pointer gamut for the corresponding hue.

The comparatively poor performance of the red coating compared to the green and blue MDMD coatings is not straightforward, but arises because of the close overlap between the sensitivity curves of the L and M cones of the human eye (see Section 1 of the Supporting Information for further discussion). Indeed, the generation of high-chroma pure red coatings is a known challenge in MDMD stack designs.^[4] In addition, the chroma of our red coating exceeded those reported elsewhere using this stack type.^[20,29]

The xy coordinates of the three coatings in comparison with the Pointer gamut are shown in Figure 1b. In terms of xy chromaticity, all three coatings lie on or are within the boundaries of the Pointer gamut, indicating that although they have higher chroma, the coatings do not have superior color purity to the colors measured in the Pointer gamut. The additive gamut defined by the coatings is a triangle covering a wide range of hues. This indicates that when used as additive primaries – for example, as RGB pixels in a reflective display – the red, green, and blue coatings can generate a gamut containing many intermediate hues of appreciable luminance and chroma.

4.3. The MDMD Coatings Still Fall Short of the Theoretical Ideal Reflectors

To further evaluate the chroma coordinates of the MDMD coatings and investigate whether additional gains can be achieved

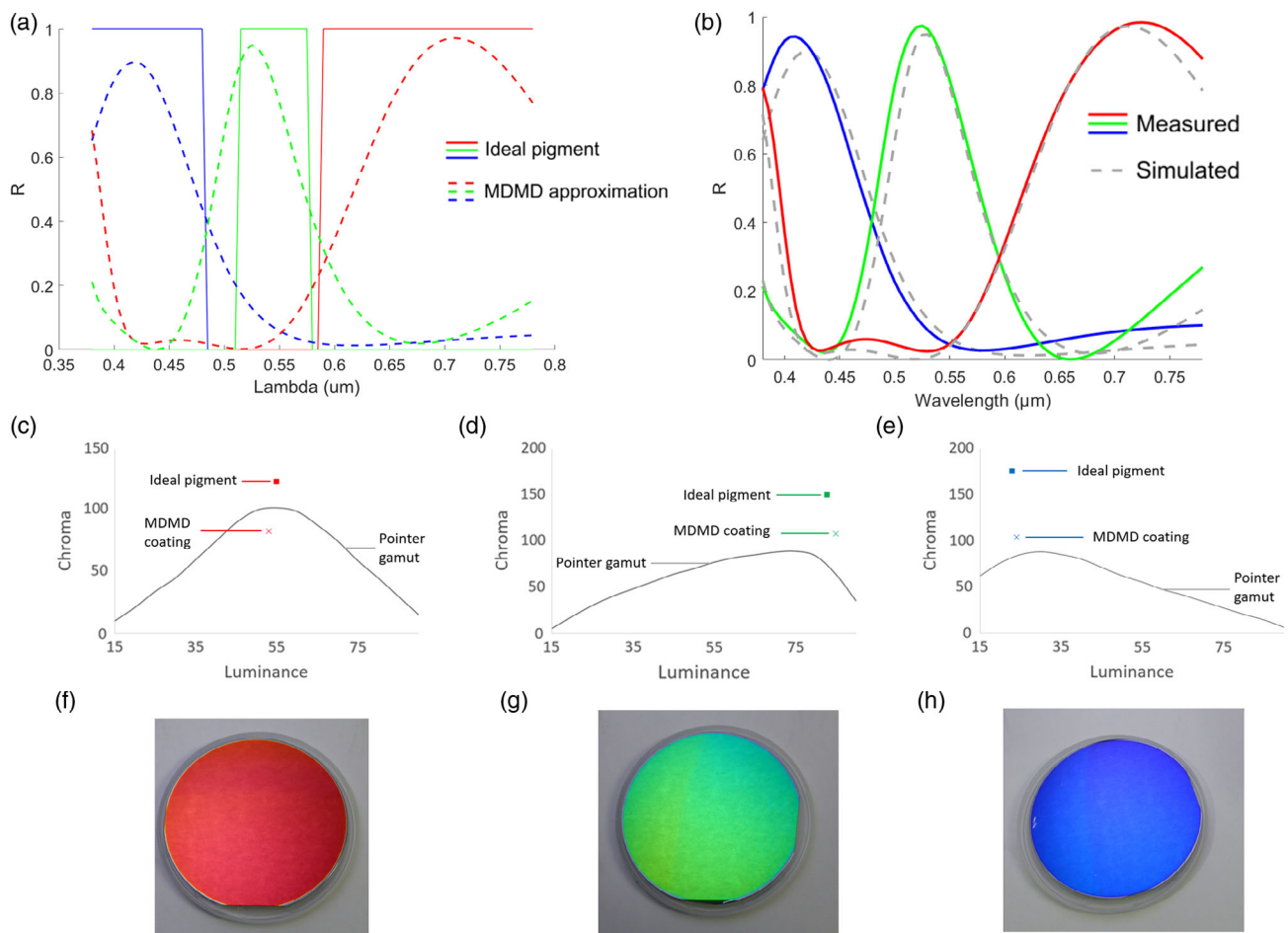


Figure 4. a) Solid: spectra of ideal red, green, and blue pigments. Dashed: simulated MDMD designs for red, green and blue coatings. b) Solid: measured reflectance spectra of red, green, and blue MDMD coatings. Dashed: the simulated spectra of the coatings, identical to those seen in (a). c–e) The luminance and chroma for the red, green, and blue (respectively) MDMD design and ideal pigment, plotted against the Pointer gamut for the corresponding hue angle. f–h) Photographs of the red, green, and blue coatings on 3" polished Si wafers. The samples appear textured owing to reflecting the illumination source, a ring light held behind a white paper diffuser. In person, the color is uniform.

using a more complex structure, the coatings were compared against the corresponding theoretical ideal reflector with the maximum possible chroma (Section 2.3). Ideal reflectors were designed to provide the same hue and luminance as the MDMD coatings under a C illuminant to within five hue degrees/luminance units, and the resulting chroma is recorded in Table 2.

In all cases, the theoretical ideal reflector chroma exceeded that of both the MDMD coating and the limits of the Pointer gamut. For the red coating, the ideal reflector demonstrated a chroma of 123, which was ≈ 20 points higher than the limit of the Pointer gamut for this hue. In comparison, the ideal reflectors for hues of 130° and 310° yielded chromas of 150 and 175, respectively, which far exceeded the limits of the Pointer gamuts for these hues.

Quantifying the perceptual difference between MDMD and ideal coatings, if they could be manufactured, is not straightforward. One option is to consider the maximal chroma achieved in the CIELAB system, which is generated by spectrally pure light

falling on a broadband reflector. For monochromatic red light at 680 nm, the perceptual chroma in CIELAB is 180. For green light at 550 nm, the chroma is 200, and for blue light at 440 nm, the chroma is 134. Thus, the appearance of the blue ideal reflector has a higher apparent chroma than monochromatic blue light, probably because of the increased apparent luminance of the coating, as it reflects a portion of the light that the eye has a greater sensitivity to.

CIELAB is nominally a perceptual color space – that is, the distance between the coordinates should be approximately linear with regard to the perceived distance between them. However, it is not uniformly perceptual, and it is difficult to infer whether a color with 200 chromas may be considered “twice as saturated” as a color with 100 chromas. Furthermore, it may be assumed that increasing chroma has diminishing returns. Certainly, the variety of pigments, paints, and inks that we encounter in everyday life is not generally considered to be somehow lacking in saturation, despite theoretically falling short of the “ideal” reflectors. Therefore, it may be sufficient to conclude that for

most observers, the limits of the Pointer gamut represent colors that are perceived as very bright and vivid; therefore, coatings that are close to or even exceed this gamut are likewise perceived as possessing outstanding brightness and saturation.

In practice, the manufacture of coatings with spectra close to those of the ideal color reflectors is extremely difficult, requiring tens or even hundreds of very thin layers whose thickness and refractive index must be precisely controlled to an exact degree. From this perspective, the MDMD coatings represent a trade-off between the complexity of the design and the resulting chroma. Although the design is simple and stable, the chroma still matches or exceeds that available using the most saturated paints. Future applications must weigh the requirements of high chroma against the constraints of complex structures when designing coatings for color control.

4.4. Deposited Coatings Show Close Agreement with Simulated Spectra

The three MDMD coating designs described in Table 2 were deposited on Si substrates using electron beam evaporation and their reflectance spectra were measured (see Section 6 for details). The deposited coatings were found to be in close agreement with the simulated spectra for all three designs (Figure 4b). The maximum divergence between the measured and simulated spectra was approximately $\Delta R = 0.05$, and the shapes of the curves closely aligned, although the locations of the peaks in the spectra may differ by ≈ 15 nm. This demonstrates accurate knowledge of both the layer indices and the deposited thicknesses.

The corresponding color differences were calculated under a C illuminant using the simple Euclidean color difference formula for CIELAB (Equation (5)). The color difference between the simulated and measured coatings was 11.3 for the red coating, 13.9 for the green coating, and 11.2 for the blue coating. Typical color tolerance thresholds are $\Delta E < 2 - 5$, depending on the application, with a color difference greater than 5 denoting a color difference that is easily noticeable by an untrained observer.^[34] As such, although the spectra show good agreement, the resulting color is significantly different from that specified by the simulated coatings. For applications where more precise color control is required, this could be improved by further careful calibration of the layer indices and the deposited thicknesses for the stack.

The coatings were deposited on both rough and polished substrates. A thin (≈ 5 nm) layer of Cr was first deposited on the substrate to aid the adhesion of the lowermost Ag layer. All three coating designs adhered well to the substrates. The coatings were stable, with undetectable changes in the reflectance spectra when measured 1 h or several weeks after deposition.

5. Conclusion

An MDMD stack type that incorporates Ti as the material for the semitransparent upper mirror was described. This stack design is highly versatile and tunable and can be used to generate a wide gamut of coatings, including red, green, and blue primary colors. The obtained chroma of the resulting colors was extremely high and was close to or surpassed the limits of the Pointer gamut for

surface color. A close agreement was obtained between the simulated and measured results, showing that a limited material choice allows precise and accurate knowledge of the behavior of each layer.

6. Experimental Section

Simulation: The coatings were simulated in MATLAB using the open-source Thin Film Toolbox^[35] using the matrix transfer method. Color coordinates were determined by integrating against the CIE XYZ matching functions under the chosen illuminant, as specified by the CIE Colorimetry 3rd Edition Technical Report (CIE 15:2004^[36]).

Index Data: The refractive indices of Ti and SiO₂ were obtained from a previous characterization as described in ref. [33]. The index of the Ti layer was fitted from the data using a combined modified Drude and Forouhi–Bloomer model, and the index of the SiO₂ layer was fitted using a two-parameter Cauchy model. The refractive index of the Ag substrate was obtained from the literature and was originally available at <http://www.sopra-sa.com/indices.html>. As of 2022, these data can be found at <http://www.sspectra.com/sopra.html> (last accessed: 24th February 2022).

Deposition: The coatings were deposited using a Buhler–Leybold Optics SYRUSpro 710 electron beam (e-beam) evaporation deposition machine under a vacuum of $\approx 2 \times 10^{-7}$ mbars. 4" commercial Si wafers were used as substrates.

Cr/Ag/SiO₂/Ti/SiO₂ coatings were deposited on these substrates. The coatings utilized a thin layer of Cr before the deposition of Ag to aid the adhesion between the layer and substrate. Ag was chosen to be sufficiently thick to be opaque (150 nm), so the substrate choice and the Cr layer have a minimal impact on the overall spectrum and appearance of the coating.

The first 50 nm of each SiO₂ layer was deposited without plasma source assistance to minimize oxidation of the layer underneath (Ag or Ti). The remainder of the layer was deposited using a plasma source assistance. In addition, the SiO₂ was etched using a plasma source prior to deposition.

A quartz balance was used to monitor the thickness of the deposited layers. This typically enables an accuracy of $\approx 2\%$ for the layer thicknesses.

Measurements: The samples were measured in reflectance using a Perkin–Elmer Lambda 1050 spectrophotometer. The wavelength range was 380–780 nm with 5 nm spacing, to overlap with the illuminant and observer data from CIE. Measurements were taken at 8°, as close as possible to normal incidence.

Photography: Sample photographs were captured using a Panasonic Lumix FZ200. Photographs were captured under ambient fluorescent light with additional lighting in the form of a white LED ring light. The light was held behind a piece of white printer paper to provide a diffuse light source as reflected in the samples. Photographs were taken at $\approx 8^\circ$, as close to the normal incidence as possible, without capturing the reflection of the camera lens in the samples.

Supporting Information

Supporting Information is available from the Wiley Online Library or from the author.

Conflict of Interest

The authors declare no conflict of interest.

Data Availability Statement

The data that support the findings of this study are available from the corresponding author upon reasonable request.

Keywords

color, Fabry–Perot, thin-film coatings

Received: April 6, 2022

Revised: June 8, 2022

Published online:

-
- [1] R. W. Sanbis, *Displays* **1999**, 20, 119.
- [2] Lexus, <https://www.lexus.eu/discover-lexus/lexus-news/lc-structural-blue> (accessed: December 2019).
- [3] S. Nanosystems, <https://www.surreynanosystems.com/about/vantablack> (accessed: March 2022).
- [4] J. Wu, in *62nd Annual Technical Conf. Proc.*, Society of Vacuum Coaters, SVC, Albuquerque, US **2019**, pp. 231–245.
- [5] Y.-G. Kim, Y.-J. Quan, M.-S. Kim, Y. Cho, S.-H. Ahn, *Int. J. Precis. Eng. Manuf.-Green Technol.* **2021**, 8, 997.
- [6] J. Wu, *Integrated Photonics: Materials, Devices, and Applications III*, Vol. 9520, SPIE, Bellingham, US **2015**.
- [7] P. Hosseini, C. D. Wright, H. Bhaskaran, *Nature* **2014**, 511, 206.
- [8] W. Dong, H. Liu, J. K. Behera, L. Lu, R. J. H. Ng, K. V. Sreekanth, X. Zhou, J. K. W. Yang, R. E. Simpson, *Adv. Funct. Mater.* **2019**, 29, 1806181.
- [9] C.-S. Park, V. R. Shrestha, S.-S. Lee, D.-Y. Choi, *Sci. Rep.* **2016**, 6, 25496.
- [10] S. S. Mirshafieyan, T. S. Luk, J. Guo, *Opt. Mater. Express* **2016**, 6, 4.
- [11] H. Song, L. Guo, Z. Liu, K. Liu, X. Zeng, D. Ji, N. Zhang, H. Hu, S. Jiang, Q. Gan, *Adv. Mater.* **2014**, 26, 2737.
- [12] J. Kim, H. Oh, M. Seo, M. Lee, *ACS Photonics* **2019**, 6, 2342.
- [13] M. A. Kats, S. J. Byrnes, R. Blanchard, M. Kolle, P. Genevet, *Appl. Phys. Lett.* **2013**, 103, 101.
- [14] Z. Dong, L. Jin, S. D. Rezaei, H. Wang, Y. Chen, F. Tjiptoharsono, J. Ho, S. Gorelik, R. J. H. Ng, Q. Ruan, C.-W. Qiu, J. K. W. Yang, *Sci. Adv.* **2022**, 8, eabm4512.
- [15] Z. Yang, C. Ji, Q. Ciu, L. J. Guo, *Adv. Opt. Mater.* **2020**, 8, 12.
- [16] A. S. Rana, M. Zubair, M. S. Anwar, M. Saleem, M. Q. Mehmood, *Opt. Mater. Express* **2020**, 10, 268.
- [17] K.-T. Lee, S. Seo, J. Y. Lee, L. J. Guo, *Adv. Mater.* **2014**, 26, 6324.
- [18] C.-S. Park, S.-S. Lee, *ACS Appl. Nano Mat.* **2021**, 4, 4216.
- [19] C. Talagrand, G. Triggs, L. Bandhu, S. Garcia-Castillo, B. Broughton, H. Bhaskaran, P. Hosseini, *J. Soc. Inf. Disp.* **2018**, 26, 619.
- [20] Z. Yang, Y. Zhou, Y. Chen, Y. Wang, P. Dai, Z. Zhang, H. Duan, *Adv. Opt. Mater.* **2016**, 4, 1196.
- [21] P. Babington, *Erwin Schrodinger's Color Theory*, Springer International Publishing, Cham, Switzerland **2017**, ISBN 978-3-319-64619-0 978-3-319-64621-3, Ch. 6.
- [22] E. Schrodinger, *Ann. Phys.* **1920**, 367, 603.
- [23] D. H. Krantz, *J. Math. Psychol.* **1975**, 12, 304.
- [24] E. Hering, *Outlines of a Theory of the Light Sense*, Harvard University Press, Cambridge, MA **1964**.
- [25] D. Malacara, *Color Vision and Colorimetry: Theory and Applications*, SPIE Press, Bellingham, WA **2011**.
- [26] M. R. Pointer, *Color Res. Appl.* **1980**, 5, 145.
- [27] C. Li, M. R. Luo, M. R. Pointer, P. Green, *Color Res. Appl.* **2014**, 39, 442.
- [28] M. R. Pointer, <https://www.rit.edu/science/munsell-color-science-lab-educational-resources> (accessed: April 2022).
- [29] Z. Yang, C. Ji, D. Liu, L. J. Guo, *Adv. Opt. Mater.* **2019**, 7, 21.
- [30] Z. Li, S. Butun, K. Aydin, *ACS Photonics* **2015**, 2, 183.
- [31] S. S. Mirshafieyan, J. Guo, *Opt. Express* **2014**, 22, 25.
- [32] M. A. Kats, R. Blanchard, P. Genevet, F. Capasso, *Nat. Mater.* **2013**, 12, 20.
- [33] R. Shurvinton, F. Lemarchand, A. Moreau, J. Lumeau, *J. Eur. Opt. Soc.-Rapid Publ.* **2021**, 17, 29.
- [34] W. Mokrzycki, M. Tatol, *Mach. Graph. Vis.* **2011**, 20, 383.
- [35] U. Griesmann, <https://sites.google.com/site/ulfagri/numerical/thin-films> (accessed: December 2019).
- [36] E. C. Carter, Y. Ohno, M. R. Pointer, A. R. Robertson, R. Séve, J. D. Schanda, K. Witt, *Cie Technical Report: Colorimetry, 3rd ed, Technical Report CIE 15:2004*, Commission Internationale de l'Eclairage, Vienna, Austria **2004**.